B. HADAŁA*, A. CEBO-RUDNICKA*, Z. MALINOWSKI*, A. GOŁDASZ*

THE INFLUENCE OF THERMAL STRESSES AND STRAND BENDING ON SURFACE DEFECTS FORMATION IN CONTINUOUSLY CAST STRANDS

WPŁYW NAPRĘŻEŃ CIEPLNYCH ORAZ ZGINANIA PASMA NA POWSTAWANIE PĘKNIĘĆ POWIERZCHNIOWYCH WE WLEWKU CIĄGŁYM

Improvement of slab surface quality is a very important goal in continues casting process of steel. It is closely coupled with casting line productivity and tendency to increase casting speed. In such a case rapid cooling of strand surface mast be employed. It results in thermal stresses development and formation of surface cracks if casting speed, cooling conditions or the arc of casting machine are not appropriate. The strain and stress fields in continuously cast strand have been determined based on the developed thermo-mechanical model and finite element software. It allowed to calculate variation of selected criterions integrals over the hole casting line starting from solidification process in the mould and ending at cutting section. Steady solution to heat transfer equation has been used to calculate strand temperature field. Mould temperature has been calculated from the three dimensional transient model. Finite element method has been employed to build steady and transient heat transfer models. Finite element solution accuracy to the temperature field has been improved. New algorithm of the solidification heat handling has been developed to stabilize a steady solution to the heat transport equation. Damageability of the strand has been evaluated based on four fracture criterions.

Keywords: continuous casting of steel, stress state, finite element method, facture criterions

Poprawa jakości powierzchni wlewka ciągłego jest jednym z głównych celów procesu ciągłego odlewania stali. Z drugiej strony ciągła potrzeba zwiększania wydajności linii produkcyjnej poprzez zwiększenie prędkości odlewania, wymaga bardziej intensywnego chłodzenia pasma. Rezultatem takich działań jest rozwój naprężeń cieplnych oraz tendencja do powstawania pęknięć powierzchniowych we wlewku ciągłym.

Naprężenia i odkształcenia powstające w materiale określono przy użyciu modelu termomechanicznego z wykorzystaniem oprogramowania bazującego na metodzie elementów skończonych. Dzięki temu możliwym stało się wyznaczenie przebiegu zmian parametrów opisujących wybrane kryteria pękania na całej długości odlewanego pasma (od momentu krzepnięcia w krystalizatorze, aż do momentu odcinania pasma na wyjściu z maszyny COS).

W opracowanym modelu wymiany ciepła pole temperatury w odlewanym paśmie wyznaczono przy pomocy stacjonarnego rozwiązania równania wymiany ciepła. Do obliczeń pola temperatury w krystalizatorze wykorzystano trójwymiarowy model niestacjonarny. W obu przypadkach w rozwiązaniu numerycznym zastosowano metodę elementów skończonych.

Poprawę stabilności i dokładności rozwiązania pola temperatury uzyskano dzięki uwzględnieniu ciepła krzepnięcia. Podatność pasma na powstawanie defektów określono za pomocą wybranych kryteriów pękania.

1. Introduction

Solidification of steel in the continuous casting line proceeds under nonequilibrium conditions and is characterized by the large cooling rate [1,2]. These may lead to formation of defects at cast strand such as surface or internal cracks. The cracks formation affects also variation of a steel chemical composition, which is caused by elements segregation. However, casting parameters are the most important. From this reason development of surface and internal cracks is very difficult to model because the temperature, strain and stress fields have to be calculated over the casting line taking into account industrial cooling conditions. Productivity improvement of the continuous casting process is essentially limited by crack formation and it is a very important problem how to determine the conditions in which fracture may occur.

Most models of crack prediction require stress and strain fields developed in material subjected to mechani-

*   AGH – UNIVERSITY OF SCIENCE AND TECHNOLOGY, FACULTY OF METALS ENGINEERING AND INDUSTRIAL COMPUTER SCIENCE, 30-059 KRAKÓW, 30 MICKIEWICZA AV., POLAND

cal and thermal loads [3,4]. Next stage is the selection of suitable crack criterion, that let to determine the moment and the place where failure may occur. The analysis of cracks criterions let us to separate four types of criterions. To the first group belong criterions is in which crack formation is predicted on the basis of the stress field [5]. The second group is constituted by criterions based on parameters determined from strain field only [5]. To the third group criterions which are based on energy of deformation can be included [6]. The fourth group of criterions consist of other methods. Selection of a proper criterion is a difficult problem and data which are available in analysis of continuous casting process have to be considered.

2. Heat transfer model

The temperature field in the strand while cooling in the continuous casting mould and in the secondary cooling zones has been determined from steady Fourier-Kirchhoff equation

$$\int \left[\lambda \left(\frac{\partial^2 T}{\partial x^2} + \frac{\partial^2 T}{\partial y^2} + \frac{\partial^2 T}{\partial z^2} \right) + q_V - \rho c \left(v_x \frac{\partial T}{\partial x} + v_y \frac{\partial T}{\partial y} + v_z \frac{\partial T}{\partial z} \right) \right] dV = 0 \quad (1)$$

where: T – temperature, K; v_x, v_y, v_z – velocity field, m/s; λ – thermal conductivity, W/(m·K); q_v – internal heat source, W/m³; c – specific heat, J/(kg·K); ρ density, kg/m³.

In equation (1), mass movement has been simplified and the velocity component in the direction of steel flow equal to casting speed $v_z = v_o$ has been assumed. The other components of the velocity field $v_x = v_y = 0$ have been assumed.

Heat generation has been included in the model and the heat of solidification has been determined from

$$q_v = Q_s \frac{dV_s}{d\tau} \quad (2)$$

where: Q_s – heat of solidification, for steel $Q_s = 1.9 \ 10^9$ J/m³; V_s – volume fraction of a solid phase, τ – time, s.

The solution of equation (1) gives the temperature field, which should satisfied the boundary conditions on the surface of the cast strand. The boundary condition have been specified in the form of heat flux transferred from the strand surface:
to the mould

$$q_{sk} = \alpha_{sk} (T_s - T_k) \quad (3)$$

to cooling water

$$q_s = \alpha_s (T_s - T_p) \quad (4)$$

to surroundings

$$q_c = \alpha_c (T_s - T_a) = (\alpha_{ra} + \alpha_{sa}) (T_s - T_a) \quad (5)$$

where: T_s – strand surface temperature, T_p – water spray temperature, T_k – mould surface temperature from the side of strand, T_a – air temperature, α_{sk} – combined heat transfer coefficient on the strand – mould interface, α_s – heat transfer coefficient for water spray cooling, α_c – combined heat transfer coefficient for air cooling.

Combined heat transfer coefficient on the strand – mould interface for strand surface temperature T_s larger then solidus temperature T_{so}, has been assumed as a constant value α_l. This value is characteristic for each specific mould and mould powders that are used in the process. Below the solidus temperature empirical formula has been used

$$\alpha_{sk} = \alpha_r + (\alpha_l - \alpha_r) \exp^{\dfrac{T_s - T_{so}}{T_{so} - T_{za}}} \quad (6)$$

where: α_r – radiation heat transfer coefficient, T_{za} – temperature of the mould powder solidification.

The radiation heat transfer coefficient has been calculated from the following formula

$$\alpha_r = 5.67 \cdot 10^{-8} \frac{\varepsilon_s \varepsilon_k}{\varepsilon_s + \varepsilon_k - \varepsilon_s \varepsilon_k} \frac{T_s^4 - T_k^4}{T_s - T_k} \quad (7)$$

where: ε_s – emissivity of the strand surface; ε_k – emissivity of the mould surface.

Below the mould, in the secondary cooling zones strand is cooled by water sprays and the convection heat transfer coefficient α_s can be calculated from the equation [7]

$$\alpha_s = 3.15 \cdot 10^9 w_s^{0.616} \left[700 + \frac{T_s - 700}{\exp(0.1 T_s - 70) + 1} \right]^{-2.455} \cdot$$
$$\cdot \left[1 - \frac{1}{\exp(0.025 \cdot T_s - 6.25) + 1} \right] \quad (8)$$

where: – w_s water spray flux rate, dm³/(m²·s).

Empirical equation (8) can be used to calculate heat transfer coefficient for water flux rate from 0.16 to 62 kg/(m²·s). Below the water spray cooling zones the strand loses heat to surroundings by radiation and convection. The radiation heat transfer coefficient α_{ra} can be calculated from:

$$\alpha_{ra} = 5.67 10^{-8} \varepsilon_s \frac{T_s^4 - T_a^4}{T_s - T_a} \quad (9)$$

For air cooling, convection heat transfer coefficient α_{sa} can be calculated from [8]

$$Nu = \frac{\alpha_{sa} \lambda_p}{L} = 0,664 Re^{1/2} Pr^{1/3} \left(\frac{Pr}{Pr_s} \right)^{0,19} \quad (10)$$

where: L – strand width, λ_p – air conductivity, Re – Reynolds number, Pr – Prandtl number calculated for surrounding air temperature, Pr_s – Prandtl calculated for air temperature equal to strand surface temperature.

The solution of the strand cooling problem is possible if mould surface temperature is known. The mould temperature has been calculated from the transient heat conduction equation

$$\frac{\partial T}{\partial \tau} = \frac{\lambda}{\rho c}\left(\frac{\partial^2 T}{\partial x^2} + \frac{\partial^2 T}{\partial y^2} + \frac{\partial^2 T}{\partial z^2}\right) \qquad (11)$$

Boundary conditions on the mould surface have been specified in the following way:
– on the inner side which is taking heat from the strand

$$q_{sk} = \alpha_{sk}\left(T_k - T_s\right) \qquad (12)$$

– on the outer side S_w cooled by water

$$q_w = \alpha_w\left(T_{kz} - T_w\right) \qquad (13)$$

where: T_w – avarage water temperature in the mould cooling channel, T_{kz} – surface temperature of the outer side of mould, α_w – heat transfer coefficient on the mould surface cooled by water. Water cooling channels are machined in mold in a form of grooves of a side length from 3 to 5 mm. Most relation for the heat transfer coefficient for turbulent flow are based on experimental studies and can be used in this case. The Nusselt number relation due to Michiejew [9] have been chosen

$$Nu = 0.021 Re_w^{0.8} Pr_w^{0.43}\left(\frac{Pr_w}{Pr_s}\right)^{0.25} \qquad (14)$$

Subscript s indicates that the Prandtl number Pr must be evaluated at the mould surface temperature and subscript w denotes that the Reynolds Re and Prandtl Pr numbers are to be evaluated at the mean bulk temperature of water. Once the Nusselt number is known the convection heat transfer coefficient for water cooling is determined from

$$\alpha_w = \frac{Nu\lambda_w}{D_h} \qquad (15)$$

where:

D_h – hydraulic diameter of the water cooling channel, m,

λ_w – water conductivity, W/(m·K).

To solve the heat transfer problem finite element method has been used. By employing the weighted residuals method to equation (1) or (2), the set of linear algebraic equations has been received:

$$\left(K_{nn} + W_{nn}\right)P_n = G_n \qquad (16)$$

where: n – number of unknowns, P_n - unknown parameters.

Several numerical models can be obtained if a proper weighting and shape function are selected. In the presented model Hermitian polynomials has been used. As a result the following form of matrix K_{nn}, W_{nn} and vector G_n were received:

$$W_{ij} = \sum_{k=1}^{27}\rho^k c^k\left(v_x^k H_i\frac{\partial H_j}{\partial x} + v_y^k H_i\frac{\partial H_j}{\partial y} + v_z^k H_i\frac{\partial H_j}{\partial z}\right)D_v^k \quad (17)$$

$$K_{ij} = \sum_{k=1}^{27}\lambda^k\left(\frac{\partial H_i}{\partial x}\frac{\partial H_j}{\partial x} + \frac{\partial H_i}{\partial y}\frac{\partial H_j}{\partial y} + \frac{\partial H_i}{\partial z}\frac{\partial H_j}{\partial z}\right)D_v^k +$$
$$+ \sum_{s=1}^{6}L^s\sum_{k=1}^{9}H_i H_j \alpha^k D_s^k \qquad (18)$$

$$G_i = \sum_{k=1}^{27}q_v^k H_i D_v^k + \sum_{s=1}^{6}\sum_{k=1}^{9}H_i\left(\alpha^k T_a^k - q^k\right)D_s^k \qquad (19)$$
$$i, j = 1, ..., 64$$

where: H_i – Hermitian shape functions, T_a – ambient temperature, q – heat flux, α – heat transfer coefficient, k – Gaussian integration point, D_V – determinant of element transformation, D_s – determinant of the element side transformation.

The unknown parameters P_i in Eq. (16) are temperatures and their derivatives in elements nodes. More detailed description of the method has been presented in [10].

In the presented numerical model boundary conditions can be specified in a simple way. Heat transfer coefficient α in equation (18) and (19) should be replaced by the value calculated from the boundary condition model described above. The ambient temperature T_a in equation (19) is equal to the mould surface temperature, the temperature of cooling water or air temperature. Solidification heat handling is more complicated. Volume fraction of a solid phase can be determined by from various models, which let us to obtain more or less accurate description of the internal heat source. In the model following equation has been used

$$V_s = 1 - \exp^{-K\frac{T_{li}-T}{T_{li}-T_{so}}} \qquad (20)$$

where: K – solidification kinetics constant, T_{li} – liquidus temperature.

The first derivative of solid volume fraction with respect to time in equation (2) can be replaced by the finite difference form:

$$q_v = Q_s\frac{\Delta V_s}{\Delta \tau} \qquad (21)$$

Scheme defined by equation (21) is usually used in finite element models. However, in case of steady solution these scheme is not satisfactory. The internal heat source

q_V have to be calculated in a different way. The following material derivative have been employed

$$\frac{dV_s}{d\tau} = \frac{\partial T}{\partial x} \frac{\partial V_s}{\partial T} \frac{\partial x}{\partial \tau} \qquad (22)$$

where:

$$\frac{\partial V_s}{\partial T} = -\frac{K}{T_{li} - T_{so}} \exp^{-K\frac{T_{li}-T}{T_{li}-T_{so}}} \qquad (23)$$

Substitute equation (22) to (2) new numerical scheme is obtained

$$q_v = -Q_s \frac{\partial T}{\partial x} v_o \frac{K}{T_{li} - T_{so}} \exp^{-K\frac{T_{li}-T}{T_{li}-T_{so}}} \qquad (24)$$

In Eqn. (22) x represents distance measured along the particle path and v_o is particle velocity. It should be noted that Eqn. (24) adds additional term to the heat load vector G. In the case of Eqn. (21) additional term has been added to the heat convection matrix W. It has significant influence on stability of the numerical solution [11].

3. Stress and strain model

In the casting machine, the cast strand is subjected to thermal and mechanical loads, which are caused by the non uniform temperature field and the set of guiding rolls. These rolls force strand movement along the casting machine arc. It causes bending and unbending of the cast strand. Local deformations that occur at the rolls – strand contact zones have been neglected in the developed stress model. Also, the influence of the gravity forces on the mean stress has been neglected. Neglecting local deformations which may be caused by rolls and gravity forces movement of the cast strand has been described by the velocity field:

$$v_1 = 0 \qquad (25)$$

$$v_2 = \omega r cos\varphi \qquad (26)$$

$$v_3 = -\omega r sin\varphi \qquad (27)$$

In the assumed co-ordinate system x_1 coordinate is directed along the axis of guiding rolls. Coordinate x_2 is perpendicular to the strand surface and coordinate x_3 is directed in line with gravity forces. Origin of the coordinate system has been fixed at the center of the meniscus as shown in Fig. 1. Cylindrical coordinates r,ϕ,z are related to Cartesian coordinates by the equations:
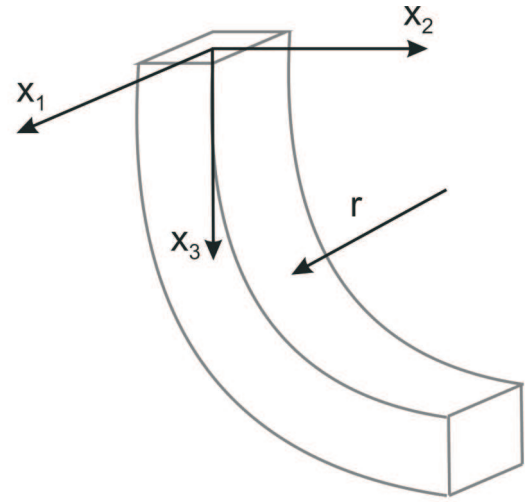

Fig. 1. Scheme of the coordinate system assumed for calculations of the stress and deformation tensors of the continuously cast strand

$$x_1 = z \qquad (28)$$
$$x_2 = r \cos\varphi - R_k \qquad (29)$$
$$x_3 = r \sin\varphi + L_k \qquad (30)$$

where: R_k – average arc radius of casting machine, L_k - length of the straight part of strand measured from the meniscus level to the inlet plane of the circumferential flow of strand, r – radius of a material point in the circumferential flow.

Angular velocity ω of the material point is calculated from the equation

$$\omega = \omega_0 + \frac{8}{\pi}(\omega_s - \omega_0)\varphi_z \qquad (31)$$

Angle φ_z is related to the coordinate φ by the following equations:

$$\varphi_z = \begin{cases} \varphi \in \left(0 \leqslant \varphi \leqslant \frac{\pi}{4}\right) \\ \frac{\pi}{2} - \varphi \in \left(\frac{\pi}{4} \leqslant \varphi \leqslant \frac{\pi}{2}\right) \end{cases} \qquad (32)$$

Angular velocity of a material point in the axis of symmetry of a cast stand is denoted as ω_s. Angular velocity of a material point at the inlet plane of the circumferential flow is denoted as ω_o.

The components of the rate of deformation tensor d_{ij}

$$d_{ij} = \frac{1}{2}\left(\frac{\partial v_i}{\partial x_j} + \frac{\partial v_j}{\partial x_i}\right) \qquad (33)$$

caused by the circumferential flow of a cast strand has been calculated as partial derivatives of the velocity field

$$\frac{\partial v_2}{\partial x_k} = -\frac{\partial \omega}{\partial x_k} r \sin\varphi - \frac{\partial r}{\partial x_k}\omega \sin\varphi - \frac{\partial \varphi}{\partial x_k}\omega r \cos\varphi,$$

$$k = 2,3 \qquad (34)$$

$$\frac{\partial \upsilon_3}{\partial x_k} = -\frac{\partial \omega}{\partial x_k} r \cos\varphi + \frac{\partial r}{\partial x_k}\omega\cos\varphi - \frac{\partial\varphi}{\partial x_k}\omega r\sin\varphi,$$

$$k = 2,3$$

(35)

Increments of the logarithmic strain tensor $\Delta\varepsilon_{ij}$ resulted from elastic-plastic bending of a strand and non uniform temperature field have been calculated from

$$\Delta\varepsilon_{ij} = \Delta\tau d_{ij} + \Delta\varepsilon_{ij}^c \tag{36}$$

The logarithmic strain tensor components have been obtained by adding up increments of strain tensor starting from the meniscus level and following the material flow up to the cut-off zone

$$\varepsilon_{ij}^{(\tau+\Delta\tau)} = \Delta\varepsilon_{ij} + R_{ik}\varepsilon_{kl}^{\tau}R_{jl} \tag{37}$$

where: $\Delta\tau$ – time increment necessary for the material point to reach the next node of element in the cross section of a cast strand. The rotation tensor is calculated from the equation

$$R_{ij} = \delta_{ij} + sin\left(\Delta\tau\omega_{ij}\right) \tag{38}$$

where: δ_{ij} – elementary tensor.

The stress tensor components have been calculated in the similar way

$$\sigma_{ij}^{(\tau+\Delta\tau)} = \Delta\sigma_{ij} + R_{ik}\sigma_{kl}^{\tau}R_{jl} \tag{39}$$

Relationships between increments of the stress tensor $\Delta\sigma_{ij}$ and the strain tensor $\Delta\varepsilon_{ij}^c$ as well as the method of thermal strains calculation have been presented in [12].

4. Crack criterion

To analyze damageability of cast strand four crack criterion have been selected [13]

1. *Plastic work criterion*

$$C_{EP} = \int_0^t \dot{\bar\varepsilon}\bar\sigma dt \quad \text{for} \quad \sigma_m > 0 \tag{40}$$

where: $\dot{\bar\varepsilon}$ – effective strain rate, $\bar\sigma$ – effective stress.

The criterion assumes that cracks will occur if strain energy is higher than the critical value C_{EP}. Plastic strain energy is calculated only at points where mean stress is positive.

2. *Rice and Tracy criterion*

$$C_{RT} = \bar\varepsilon\exp\left(-\frac{3}{2}\frac{6m}{\bar\sigma}\right) \tag{41}$$

where: σ_m – mean stress, $\bar\varepsilon$ – effective strain.

Rice and Tracy criterion predicts that failures will form if parameter C_{RT} passes the critical value of the effective strain $\bar\varepsilon_f$

3. *Modified Rice and Tracy criterion*

Modification of Rice and Tracy criterion (41) rely on calculating the critical value of C_{RM} parameter, as a sum of right side of equation (41). The summation is made only at points for which the mean stress is positive.

$$C_{RM} = \sum\Delta\bar\varepsilon\exp(-\frac{3}{2}\frac{\sigma_m}{\bar\sigma}) \quad \text{for} \quad \sigma_m > 0 \tag{42}$$

4. *Latham criterion*

$$C_{LO} = \int_0^t \sigma_{max}\dot{\bar\varepsilon}\ dt \quad \text{for} \quad \sigma_m > 0 \tag{43}$$

where: σ_{max} – maximum stress.

Latham criterion assumes cracks formation if strain work done by the maximum tensile stress passes the critical value C_{LO}. The uniaxial tension test can be employed in order to determine the critical values of C_{EP}, C_{RT}, C_{LO} parameters for a particular steel.

5. Numerical calculations

The influence of strand temperature field and the circumferential flow of a cast strand along the arc of casting machine on the strain and stress development have been analyzed for the square strand of 160mm×160mm. Chemical composition of steel has been assumed for the calculation as: C=0.1%, Mn=1.7%, Si=0.39%, Cr=3.0%, Ni=0.2%. Thermophysical properties of steel were selected on the ground of steel chemical composition. In Figures from 2 to 8 heat conduction coefficient, density, specific heat, Young's modulus, flow stress, Poisson's ratio and thermal expansion coefficient as a function of temperature for the steel employed in computations have been presented.
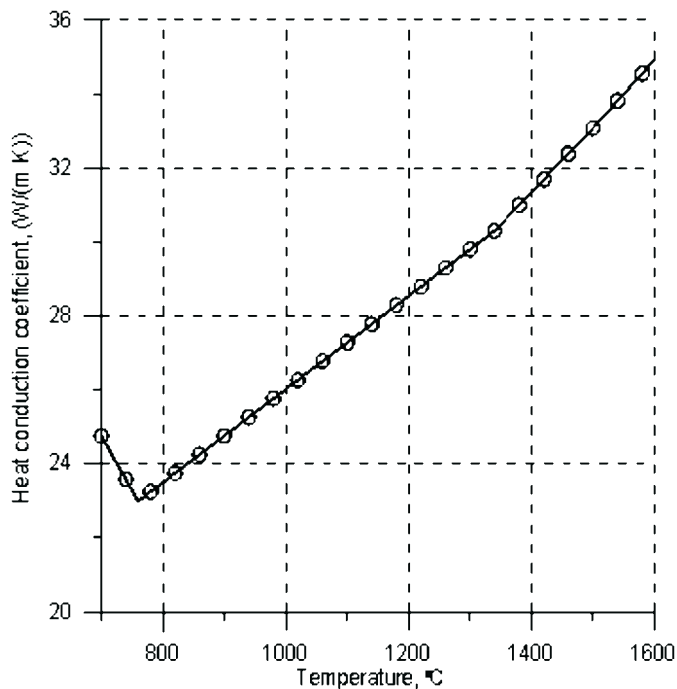
372

Fig. 2. Heat conduction coefficient as a function of temperature for the steel employed in computations
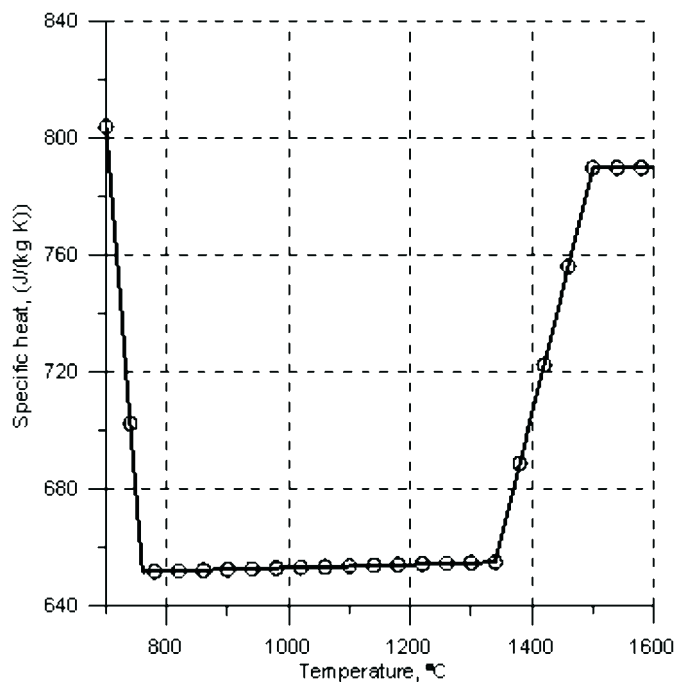

Fig. 4. Specific heat as a function of temperature for the steel employed in computations
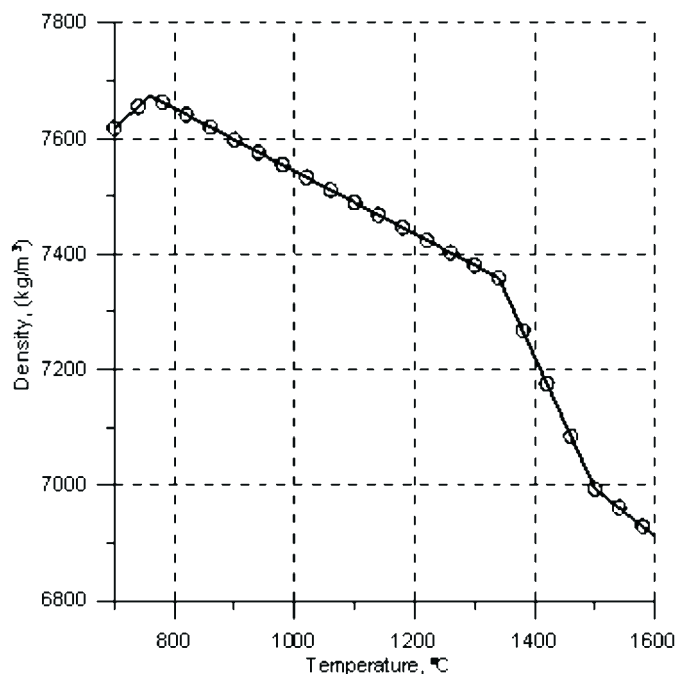

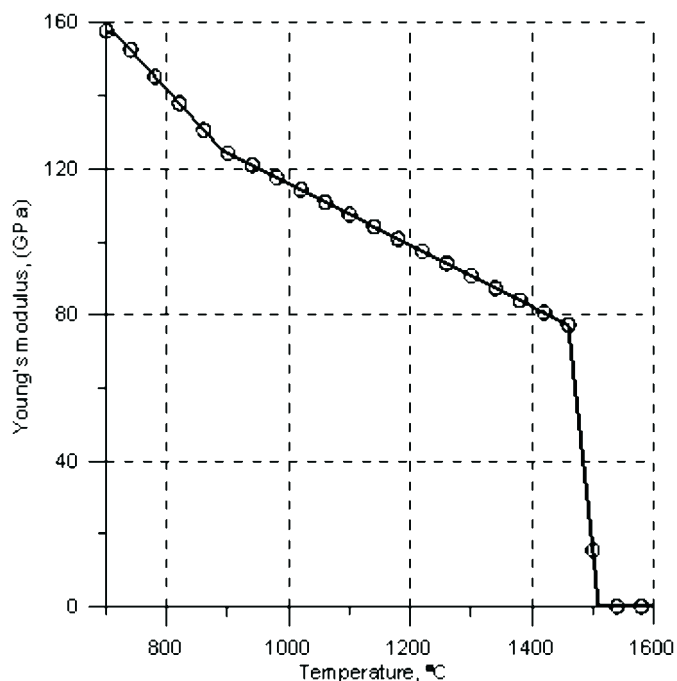Fig. 3. Density as a function of temperature for the steel employed in computations

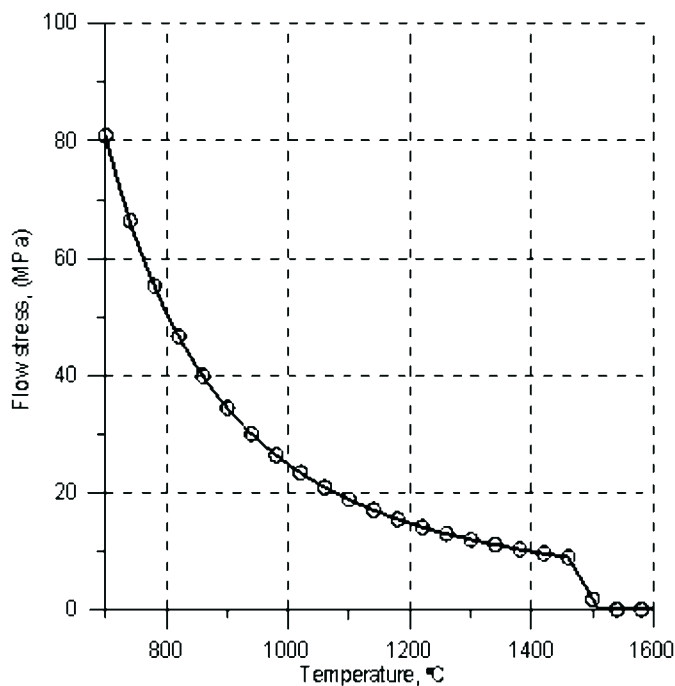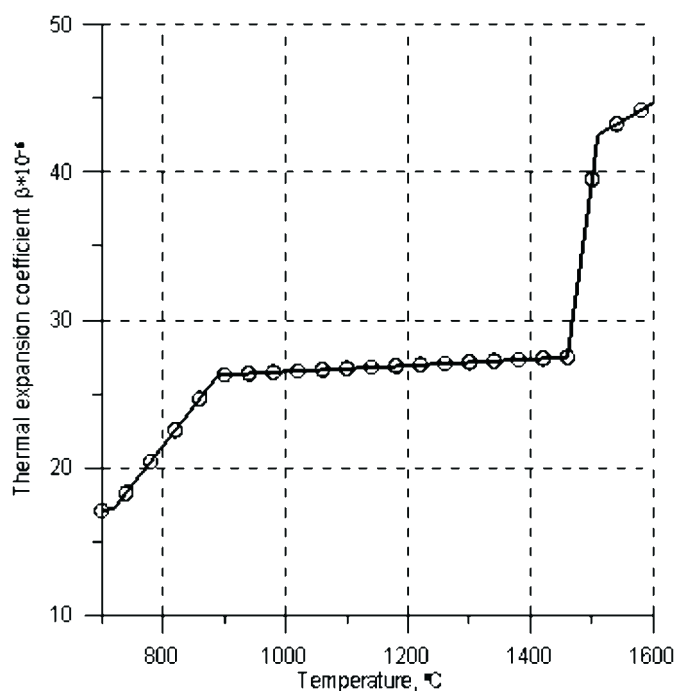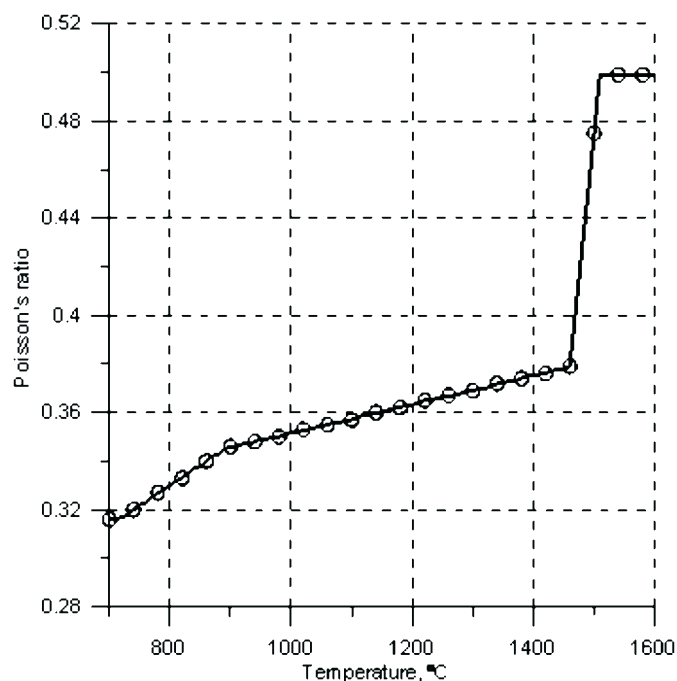Fig. 5. Young's modulus as a function of temperature for the steel employed in computations

Fig. 6. Flow stress as a function of temperature for the steel employed in computations

Fig. 8. Thermal expansion coefficient as a function of temperature for the steel employed in computations

Solidus temperature was assumed as 1460°C, liquidus as 1510°C. In the solid state the austenitic transformation boundaries were assumed as: 890°C and 720°C. The analysis has been performed for the arc of casting machine equal 6 m. Casting speed was assumed as 1,8 m/min. The length of the secondary cooling zone was equal 4,51 m. Computation have been performed for the following cases:

- Case I – bending and unbending of the cast strand only. Thermal strains have been removed from the strain tensor in order to examine the influence of the circumferential flow of strand only.
- Case II –thermal stresses only. The influence of the circumferential flow of the strand has been neglected.
- Case III – coupled effect of the stress and strain field resulting from non uniform temperature field and the circumferential flow of the cast strand.

In Fig. 9 temperature distribution in the axis of cast strand, in the axis of the strand side surface and in strand corners have been presented. The results have been obtained for the heat source given by equation (21). Estimation of the derivative of the solidification heat by the finite difference scheme, did not give stable solution. In Fig. 9 decrease in cast strand temperature below the ambient temperature is observed in range of 2 m from the meniscus level. Temperature distribution does not reflect temperature obtained in real process. New scheme of the internal heat handling defined by equation (24) resulted in a very good stability and accuracy of the finite element model.

Fig. 7. Poisson's ratio as a function of temperature for the steel employed in computations

From the heat balance calculated for the control volume [14] follows, that the standard weighted residuals method gives the strand temperature of about 225°C too low. The correct solution has been obtained after iterative modification of weighting function H_i in equation (18). The correction factor has been employed for scaling the weighting function, has been calculated from the heat balance. The developed numerical scheme is stabile and efficient. Temperature distributions at side surface of the cast strand and at its corners presented in Fig. 10 and 11, do not indicate any oscillations. Noticeable at these figures increses and decreases of the strand temperature result from the changes in cooling conditions in the subsequent cooling zones. The final, smooth parts of the temperature distributions reflect strand cooling in air.

Fig. 11. Distribution of the temperature in the corner of the continuously cast strand for the solidification heat given by Eq. (24)

Fig. 9. Temperature distributions at selected points of the continuously cast strand for the solidification heat given by Eq. (21)
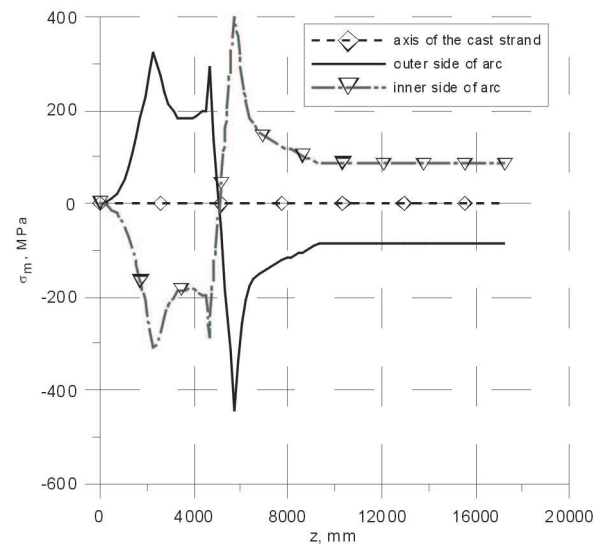
Fig. 12. Average stress distributions at selected points of the continuously cast strand resulting from bending of the strand

In Fig. 12 to 15, the results of calculation of the effective strain and mean stress have been presented. In the case of mean stress the results have been presented for characteristic points of a cast strand cross section. Effective strain in 2 selected cross section of the cast strand has been presented: below casting mould and after unbending of the strand.

Analysis of the mean stress distribution, resulted from bending of a cast strand (Fig. 12) leads to conclusion, that in the cast strand axis mean stress is equal zero. The outer surface of a cast strand is tensiled to the half of the length of arc of casting machine. Then, the mean stress turns to positive values. In the same time the mean stress distributions on the strand surface from the inner side of arc of casting machine show opposite
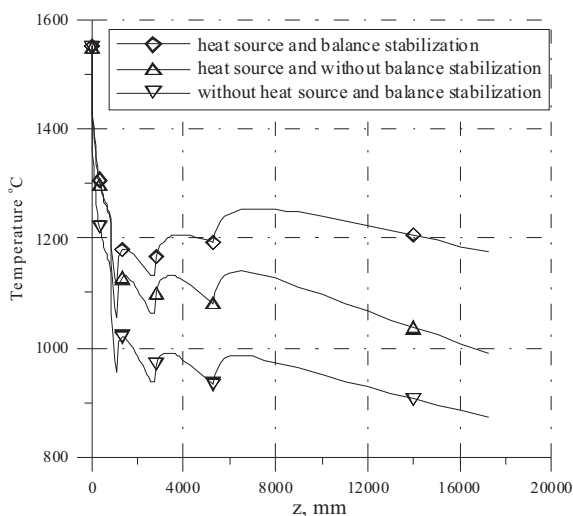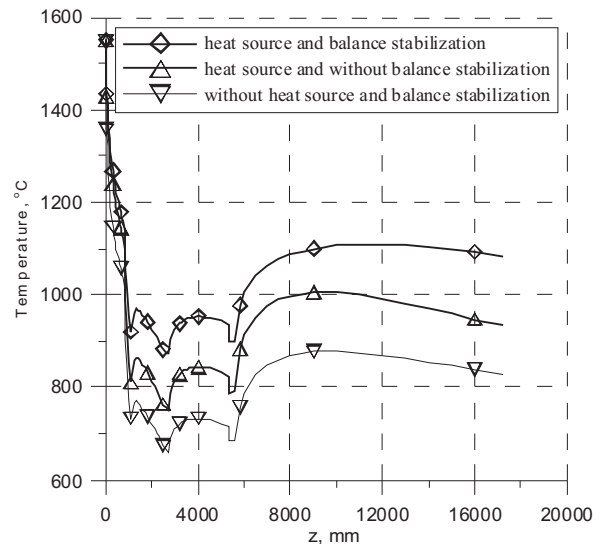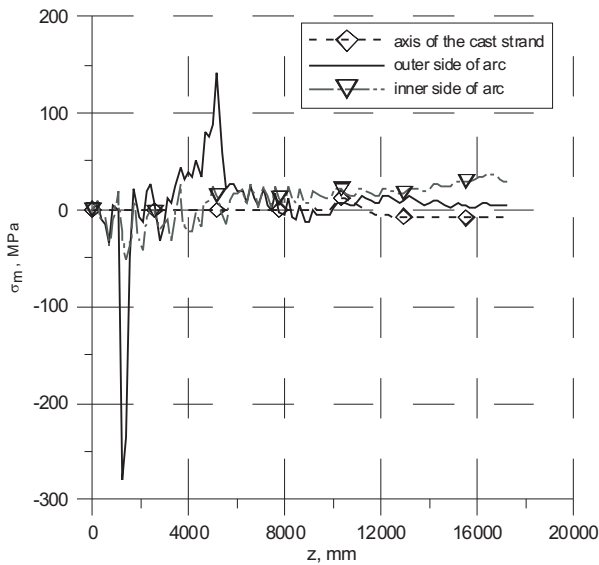

Fig. 10. Distribution of the temperature on the side surface of the continuously cast strand for the solidification heat given by Eq. (24)

Fig. 13. Average stress distributions at selected points of the continuously cast strand resulting non uniform temperature field

distribution is affected by bending of a cast strand. The mean stress (Fig. 13) caused by non uniform temperature field, changes the distributions of mean stress (Fig. 14), but the curves follow the results of the bending model. The highest values of the mean stress in case of corners of a cast strand have not exceeded ±400 MPa (Fig. 14).
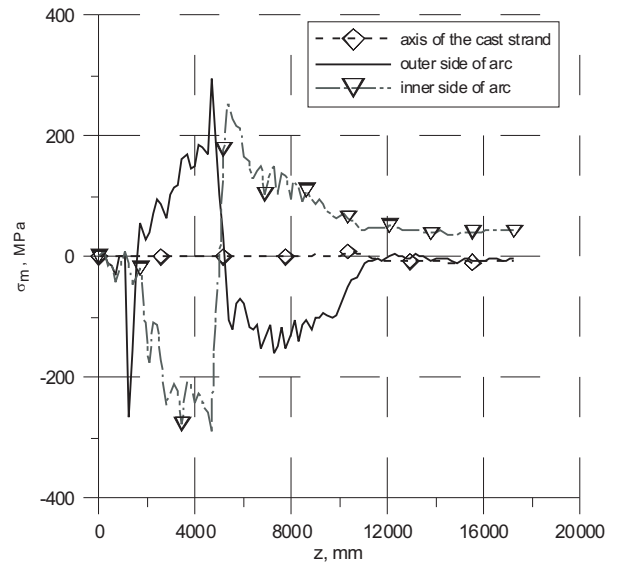

Fig. 14. Average stress distributions at selected points of the continuously cast strand resulting from non uniform temperature field and the strand bending

behavior. Stress distributions are symmetrical and characteristic for bedning of a cast strand. The surface of a cast strand passes to the plastic state as a result of deformation caused by bending of a cast strand. Further deformation of a cast strand is caused by non uniform temperature field. In Fig. 15 the total effect of these two factors on the effective strain is presented. Effective strain reaches 0.06 at the surface layers. Mean stress
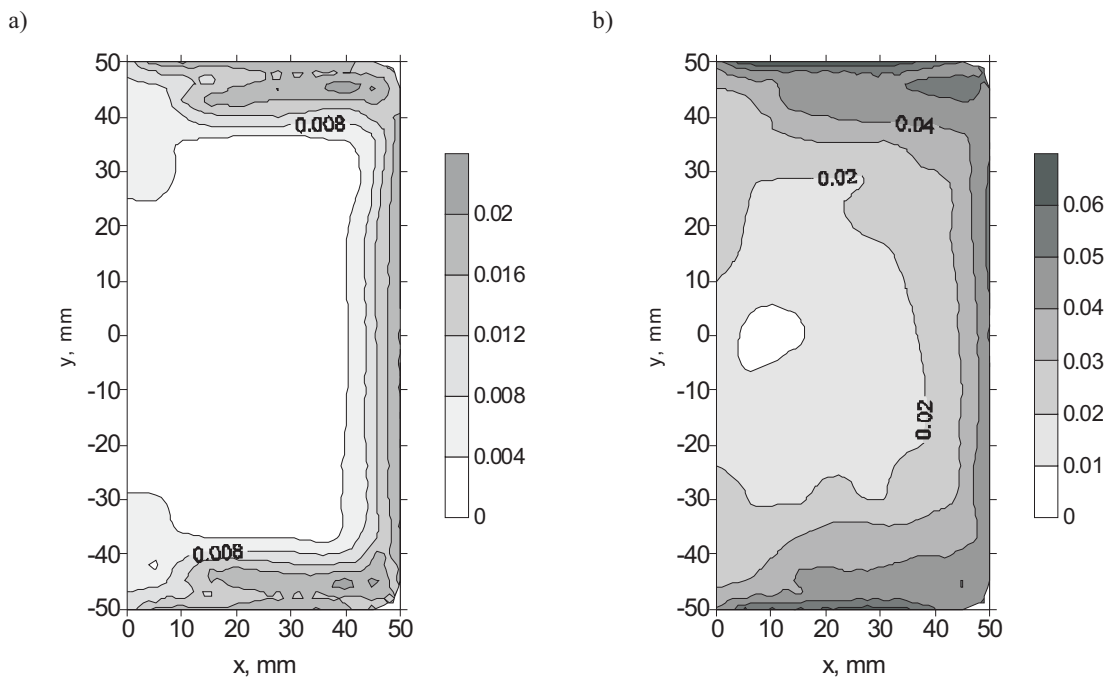
a)

b)

Fig. 15. Effective strain distributions in the cross section of the continuously cast strand resulting from the strand bending and non uniform temperature field. a) below the mould, b) after the strand straightening

Calculated values of crack criterion parameters confirmed that the most susceptible to crack formation are corners of the cast strand. Analysis of the results of Rice and Tracy criterion do not give the possibility to identify zones cracks formation. Values of these criterion for outer corner of a cast strand are much higher than that obtained for inner corner and strand axis. Unfortunately on all those curves peaks are noted (Fig. 16). It makes the proper interpretation of the results very difficult. This problem disappears after modification of Rice and Tracy criterion. Results of calculations given by plastic work and Latham criterions indicated as the most probable place of crack formation zones between the 1st and the 5th meter of the outer corner of the cast strand (Fig. 18, 19). It is the bending zone. In case of inner corner of a cast strand potential fractures may occur after leaving the casting mould (at about 1th meter of the metallurgical length of strand) and then again in unbending zone (between 5th and the 8th meter of the metallurgical length of strand). In these regions parameters calculated from plastic work and Latham criterions increase very rapidly. Similar domains are indicated by modified Rice and Tracy criterion (Fig. 17). Such a course of curves is justifiable by thermal and mechanical loads.
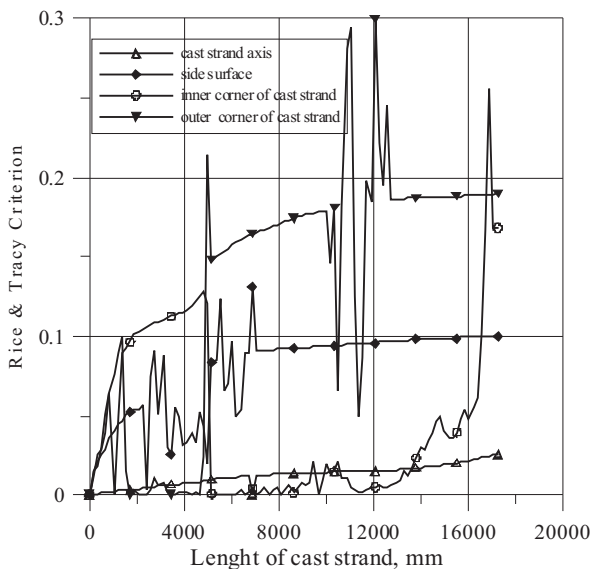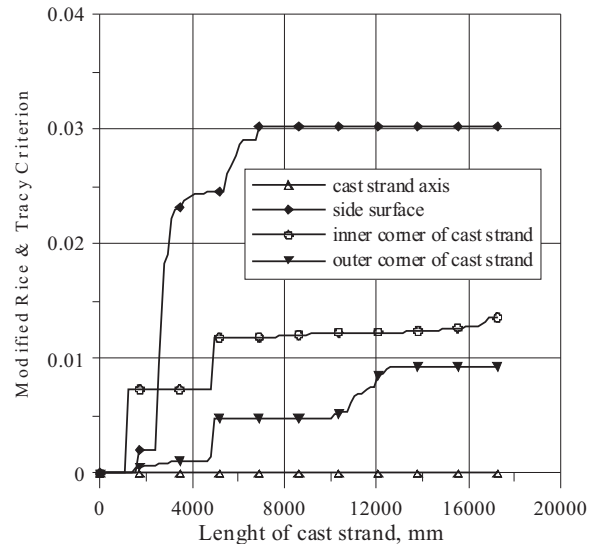

Fig. 17. Results of calculations of the modified Rice and Tracy criterion

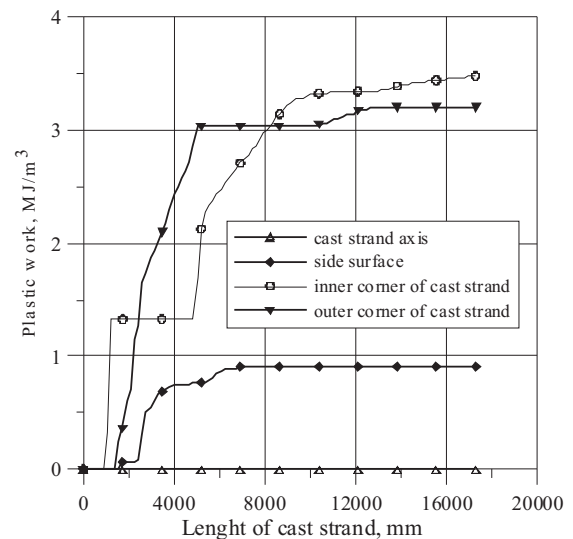Fig. 18. Results of calculations of strain criterion

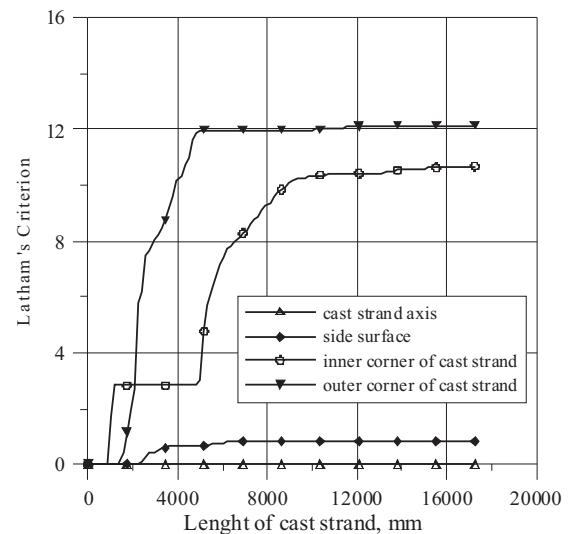Fig. 16. Results of calculations of Rice and Tracy criterion

Fig. 19. Results of calculations of Latham criterion

6. Conclusions

New, stable scheme of solidification heat handling in steady solution of heat transfer model has been developed. The strain and stress field in the continuously cast strand, have been determined. The accuracy of thermal model has been improved based on the heat balance calculated in control volume. Iterative scaling of weighting function in the weighted residual method let to obtain stable and accurate solution. The possibility to analyze the influence of casting parameters on the temperature, strain and stress fields is possible. The largest influence on the mean stress has bending and unbending of a cast strand. The highest values of mean stress in these case reach about ±400 MPa. Dominant influence on the effective strain distribution has the non uniform temperature field. The domains of maximal deformations are located near the surface of a cast ingot. Along the whole casting line the lowest values of the effective strain occur at the axis of the cast ingot.

The calculations performed for selected crack criterions let to identify the domains most exposure to cracks formation and development. The most useful are strain work criterion, Latham criterion and modified Rice and Tracy criterion. Numerical calculations performed on the basis of these three criterions indicated the same regions of possible cracks formation as that well known from the industrial practice. It is necessary to employ uniaxial tension tests to determine critical values of fracture criterion parameters. Unfortunately, uniaxial tension tests have to be conducted in a very wide range of temperatures.

REFERENCES

[1] M. G o n z a l e z, M.B. G o l d s c h m i t, A.P. A s - s a n e l l i, E. F. B e r d a g u e r, E.N. D v o r k i n, Modeling of the Solidification Process in a Continuous Casting Installation for Steel Slabs, Metallurgical and Materials Transactions B **34**, 4, 455-473 (2003).

[2] B. G. T h o m a s, Modeling of the continuous casting of steel – past, present and future, 59th Electric Furnace Conference Proceedings, Pheonix, Iron & Steel Society, 3-30 (2001).

[3] B.C. L i u, J.W. K a n g, S.M. X i o n g, A study on the numerical simulation of thermal stress during the solidification of shaped castings, Science and Technology of Advanced Materials **2**, 157-164 (2001).

[4] J.E. L e e, T.J. Y e o, K.H. O h, J.K. Y o o n, U.K. Y o o n, Prediction of cracks in continuously cast steel beam blank through fully coupled analysis of fluid flow, heat transfer and deformation behavior of solidifying shell, Metall. Trans. A **31A**, 225-237 (2000).

[5] W. M. G a r r i s o n Jr, Ductile fracture, J. Phys. Chem. Solids **48**, 11, 1035-1074 (1987).

[6] Y.M. W o n, T.J. Y e o, D.J. S e o l, K.H. O h, A new criterion for internal crack formation in continuously cast steels, Metall. Trans. B **31B**, 779-794 (2000).

[7] P.D. H o d g s o n, K.M. B r o w n e, D.C. C o l l i n s o n, T.T. P h a m, R.K. G i b b s, Proc. 3rd Int. Semin.on Quenching and Carburising, Melbourne, 139, (1990).

[8] A.Ç. Y u n u s, Heat and mass transfer, McGrawHill, New York (2007).

[9] S. W i ś n i e w s k i, T. S. W i ś n i e w s k i, Wymiana ciepła, Wydawnictwa Naukowo Techniczne, Warszawa, (1994) (in Polish).

[10] B. H a d a ł a, Z. M a l i n o w s k i, Accuracy of the finite element solution to steady convection-diffusion heat transport equation in continuous casting problem. Informatyka w Technologii Materiałów **9**, 2, 302-307 (2009).

[11] B. H a d a ł a, Z. M a l i n o w s k i, A. G o ł d a s z, A. C e b o - R u d n i c k a, Effect of the solidification heat on the strand temperature field in the continuous casting, Hutnik, R. **77** 11, 636-639 (2010) (in Polish).

[12] Z. M a l i n o w s k i, Numeryczne modele w przeróbce plastycznej i wymianie ciepła, Uczelniane Wydawnictwa Naukowo – Dydaktyczne, Kraków (2005) (in Polish).

[13] A. C e b o - R u d n i c k a, Z. M a l i n o w s k i, A. G o ł d a s z, M. R y w o t y c k i, Application of fracture criterions to cracks prediction of the continuously cast strand, Hutnik, R. **77**, 11, 646-649 (2010) (in Polish).

[14] A. G o ł d a s z, Z. M a l i n o w s k i, B. H a d a ł a, Study of heat balance in the rolling process of bars, Archives of Metallurgy and Materials **54**, 3, 685-694 (2009).